Liquid Crystals
Publication details, including instructions for authors and subscription information:
http://www.informaworld.com/smpp/title~content=t713926090

A simple molecular theory of the SmA nematic lake in highly polar compounds -SmA critical point and 1 d

A. S. Govind; N. V. Madhusudana

Online publication date: 29 June 2010

To cite this Article Govind, A. S. and Madhusudana, N. V.(1997) 'A simple molecular theory of the SmA nematic lake in highly polar compounds -SmA critical point and 1 d', Liquid Crystals, 23: 3, 327 — 337
To link to this Article: DOI: 10.1080/026782997208253
URL: http://dx.doi.org/10.1080/026782997208253

LIQUID CRYSTALS, 1997, VOL. 23, NO. 3, 327–337

A simple molecular theory of the SmA_1–SmA_d critical point and nematic lake in highly polar compounds

by A. S. GOVIND† and N. V. MADHUSUDANA*

Raman Research Institute, C.V. Raman Avenue, Bangalore 560 080, India

†Department of Physics, Vijaya College, Basavanagudi, Bangalore 560 004, India

(*Received 10 January 1997; in final form 31 March 1997; accepted 8 April 1997*)

Our earlier model of liquid crystals consisting of highly polar compounds in which the molecules can form either parallel or antiparallel pairs, has been extended. Depending on the model parameters the following results are obtained: (i) first order SmA_1–SmA_d transition which changes over to a continuous SmA_1–SmA_d evolution beyond a critical point in two regimes of the McMillan α parameter, (ii) a re-entrant nematic lake associated with the SmA_1–SmA_d boundary, and (iii) the merger of the re-entrant nematic lake with the nematic sea. The results are discussed in comparison with experiments and other theoretical models.

1. Introduction

Mesomorphic compounds whose molecules have the strongly polar C≡N or NO_2 end groups exhibit a variety of interesting phase transitions. In particular, some compounds with cores having 2 or 3 phenyl rings exhibit three polymorphic forms of smectic A (SmA) namely monolayer smectic A (SmA_1), bilayer smectic A (SmA_2) and partial bilayer smectic A (SmA_d). This classification is based on the smectic layer spacing d relative to the length l of the constituent molecules. In the SmA_1 phase $d \approx l$ while $d \approx 2l$ in the SmA_2 phase. For the SmA_d phase $l < d < 2l$. Such compounds exhibit the phenomenon of double re-entrance [1], multiple re-entrance and smectic polymorphism [2, 3]. A nematic lake surrounded by the smectic phase at the termination of a first order SmA_1–SmA_d boundary has been found in some cases. (We prefer nematic 'lake' to nematic 'island' used by some authors [4] as the nematic is more fluid than the smectic.) Another observation is on the SmA_1–SmA_d line ending in a critical point beyond which there is a continuous evolution between the two phases [4–8]. Very recently, the induction of a smectic A_d island surrounded by the nematic phase has been observed in some binary mixtures [9]. Prost and co-workers have developed a successful Landau theory of these phase transitions [10–12], in which two competing order parameters give rise to the rich variety of phase diagrams. These order parameters correspond to the two incommensurate lengths, namely the molecular length l and the length l' of a suitably associated antiparallel pair of molecules such that $l < l' < 2l$.

*Author for correspondence.

There have also been several attempts to develop molecular theories of these phase transitions [13–20]. A particularly simple molecular model [20] was proposed by us to explain double re-entrance. In this model, the origin of the two incommensurate lengths is explained as follows: the permanent dipolar interaction favours an antiparallel arrangement between the neighbouring mesogenic molecules [21]. However, the aromatic part of the antiparallel neighbours overlap due to the strong dispersion interaction between them leading to the partial bilayer arrangement (see figure 1 (*a*)). In this configuration, the alkyl chains of the two molecules which lie on opposite sides of the core region, do not have a significant interaction.

On the other hand, if the molecules are parallel, the permanent dipolar interaction is repulsive. However, the aromatic cores have strong polarizabilities and the induced dipole moment due to a neighbouring polar molecule would weaken the net dipole moment of any given molecule in this configuration (see figure 1 (*b*)). Further, the chains of the two neighbours are now in close proximity and the dispersion interaction between them would favour this arrangement. The dipolar interaction is $\propto 1/r^3$ where r is the intermolecular separation, while both the dipole-induced dipole and the dispersion interactions are $\propto 1/r^6$. Hence there can be a change from the antiparallel to the parallel configuration as the intermolecular separation is decreased below some value as the density is increased, i.e. as the temperature is lowered (or as the pressure is increased). Also, the McMillan parameter α which is a measure of the layering interaction is greater for the antiparallel configuration than for the parallel configuration. Hence, compared to the SmA_d phase the SmA_1 phase undergoes a transition

0267–8292/97 $12·00

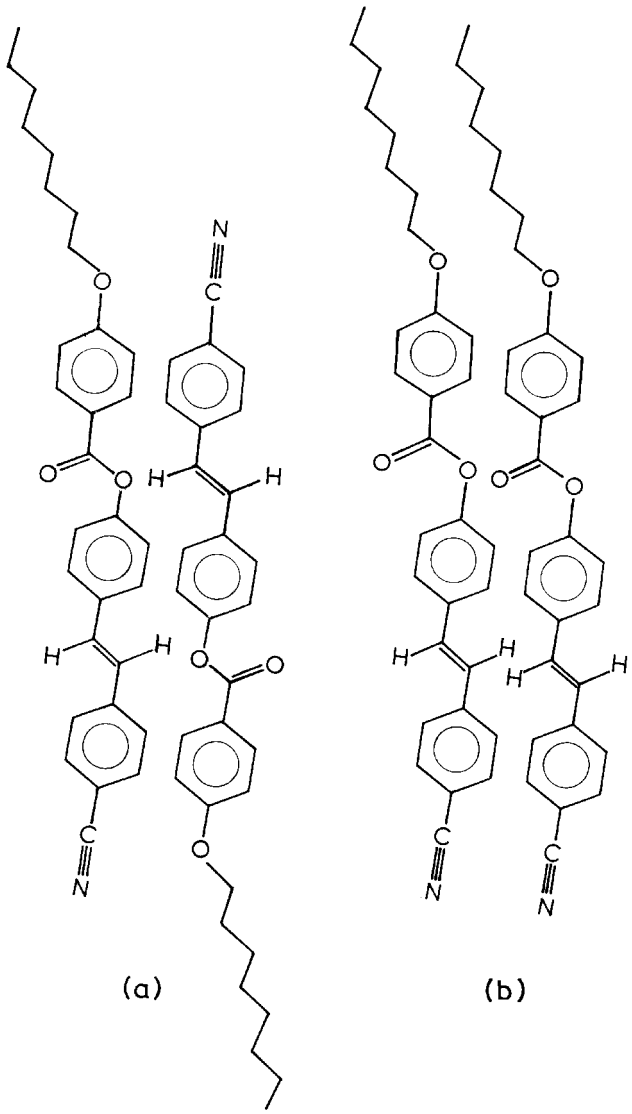

Figure 1. (*a*) The antiparallel configuration of two octyloxybenzoyloxy cyanostilbene (T8) molecules favoured at intermediate molecular separations and (*b*) the parallel configuration favoured at relatively low values of intermolecular separation (from [20]).

to the nematic phase at a lower temperature. As the temperature is lowered in the SmA_d phase, the number of pairs with parallel configuration gradually increases at the expense of antiparallel pairs. Since the SmA_1 phase with a lower value of α is stable only at very low temperatures, the nematic phase re-enters. The SmA_1 phase itself becomes stable on further cooling. In other words, we get the double re-entrant sequence N–SmA_d–R_N–SmA_1 as explained in [20].

In an earlier paper [22], we have extended the above model to predict the possibility of a nematic to nematic transition. In that paper, only the orientational interaction energy was considered. The relative concentration of the molecular pairs with the two configurations jumps at some temperature leading to a weak first order phase transition with a large variation of specific heat in a narrow range of temperatures around the transition point. The transition disappears above a critical point, as expected, since the two nematic phases have the same symmetry.

In the present paper, we extend this model [22] to explain the SmA_1–SmA_d transition. For the sake of simplicity, we assume that the nematic order is saturated, i.e. $S=1$. Depending on the values of the parameters used, our calculations show the possibility of (i) a first order SmA_1–SmA_d transition changing to a continuous SmA_1–SmA_d evolution beyond a critical point, (ii) a re-entrant nematic lake associated with the SmA_1–SmA_d transition, and (iii) the re-entrant nematic lake merging with the nematic sea.

In the next section, the theoretical model is presented. In § 3, the method of calculation is explained. In § 4, the results of the calculation are discussed in comparison with experiments and other theories. Some concluding remarks are given in § 5.

2. Theoretical model

2.1. *Assumptions*

In order to simplify the theory, the following assumptions are made:

(1) As already mentioned, the nematic order it taken to be saturated and only the smectic interactions are considered.

(2) As in [20, 22], the medium is assumed to consist of 'pairs' of molecules having either antiparallel (A) or parallel (P) configurations. Frustration in orientation of a third molecule can lead to stable pairs with A-type configuration. On the other hand, a large number of molecules can be associated in the P-type configuration. However, for the sake of simplicity, we assume that even the P-type configuration consists of only pairs, as in the earlier papers [20, 22].

(3) As we described earlier, the A-type configuration is favoured at lower densities and P-type at higher densities. Again, as in [20], for the sake of simplicity, it is assumed that the energy difference between the two configurations has the following form:

$$\Delta E = E_A - E_P = R_1 kT^* \left(\frac{R_2}{T_R} - 1 \right) \qquad (1)$$

where k is the Boltzmann constant, E_A and E_P are the configurational energies of the A-type and P-type pairs, respectively, $R_1 kT^*$ is an interaction parameter and $T_R = T/T^*$ is the reduced temperature. Here T^* is some reference temperature. In [22], the nematic order is not assumed to be saturated, and we have used $T^* = T_{NI}$,

with $T_{NI} = 500$ K where T_{NI} refers to the nematic–isotropic transition temperature of the A-type of pairs. To have the same numerical value of ΔE, we take $T^* = 500$ K in the present paper. R_2 is the reduced temperature at which the density of the medium is such that ΔE becomes zero. For $T_R > R_2$, the A-type configuration has the lower energy.

(4) The McMillan parameters for A-type (α_A) and P-type (α_P) configurations can be written as

$$\alpha_A = 2 \exp(-[\pi r_o/(r_o + 2c)]^2) \quad (2)$$

and

$$\alpha_P = 2 \exp(-[\pi r_o/(r_o + c)]^2) \quad (3)$$

where r_o and c are the lengths of the aromatic and chain moieties of the molecule respectively. α_P is obviously related to α_A. The mutual interaction parameter

$$\alpha_{PA} = \alpha_{AP} = \alpha_E = Q \alpha_A \alpha_P \quad (4)$$

where $Q \neq 1$ indicates a deviation from the geometric mean rule.

(5) In the earlier papers [20, 22], ΔE was taken to be a function of temperature only (see equation (1)). But, we note that the nematic lake is found in mixtures of chemically dissimilar compounds. Hence, an exact description of this phenomenon requires a general theory of mixtures. However, for the sake of simplicity we assume that the McMillan parameter α_A (or α_P) is adequate to represent a given concentration in such mixtures. In a homologous series, the chain length of the molecule and hence α varies. The chain–chain interaction energy and hence E_P can also be expected to vary with α. We assume that $\Delta E \propto (\alpha_A)^n$ where α_A is the McMillan parameter for the A-type of pairs.

We calculate ΔE for a pair as follows. We have, for P-type of pairs,

$$\mu_p = \mu - \mu_i = \frac{\mu}{1 + \chi/r^3}$$

where μ_p is the net electric dipole moment of a molecule in the P-type configuration, μ the permanent dipole moment, μ_i the induced dipole moment, χ the polarizability of the aromatic core, and r the intermolecular separation. For the A-type of pairs, the net dipole moment is given by

$$\mu_A = \mu + \mu_i = \frac{\mu}{1 - \chi/r^3}.$$

The pairing energy for P-type of pairs is given by

$$E_p = \frac{\mu_p^2}{r^3} - KC^2$$

where K is the chain–chain interaction parameter and C is the chain length, and we have not shown the energy due to the dispersion interactions between the cores as it is supposed to be the same in the A and P configurations.

Since the chains are not in close proximity in the A-type of pairs, we have,

$$E_A = -\frac{\mu_A^2}{r^3}.$$

The following parameters are very reasonable [20] for the present calculations: $\mu = 2 \times 10^{-29}$ C m, $\chi = 20 \times 10^{-30}$ m^3. The core length corresponds to 10 carbon–carbon linkages in the chain, and $K = 1{\cdot}1 \times 10^{-75}$ SIU. Using these, ΔE is calculated for $r = 0{\cdot}45$ nm and $0{\cdot}50$ nm for various values of C. By plotting log ΔE against α_A which is given by equation (2), it is seen that the slope ≈ 4 for the range of α_A relevant in our calculations. Hence we take $\Delta E \propto (\alpha_A)^4$. Since ΔE linearly depends on the interaction parameter R_1, we assume that

$$R_1 = R_1^* \alpha_A^4 \quad (5)$$

where R_1^* is an input parameter. R_2 can also be expected to depend weakly on the chain length in a homologous series i.e. on the McMillan parameter α. We ignore this dependence of R_2 with α.

(6) As noted by Humphries and Luckhurst [23], most experimental phase diagrams on binary mixtures of nematics correspond to a negative deviation from the geometric mean (GM) rule for the mutual interaction between the components. We have shown in our earlier paper [22] that a negative deviation is necessary to get a nematic to nematic phase transition in polar compounds. Humphries *et al.*, have also shown that the deviation increases as the molecular structures of the two components become more dissimilar. This trend is also seen in the N–I transition boundaries studied by Demus *et al.* [24], in a large number of binary mixtures whose components belong to a homologous series.

We can expect a similar negative deviation in the case of mutual interaction in the smectic phase also, i.e. for the McMillan parameter α_{AP}. As we have discussed, the P-type and A-type configurations give rise to the smectic A_1, and smectic A_d phases, respectively. There have been some experiments on binary mixtures of polar compounds [25] in which one component is of type smectic A_1 and the other is smectic A_d. In these cases, the smectic–nematic transition line has an appreciable concave shape, especially when the components have a large difference in the layer spacing, indicating a strong negative deviation from the GM rule for the mutual interaction. In other words, $Q < 1$ in equation (4). As the chain length in a homologous series is increased, the numerical value of α_A as also the structural dissimilarity between the P- and A-types of pairs is enhanced. Hence

it is reasonable to assume that as α_A increases the deviation (1-Q) from GM rule increases, or Q decreases.

Since both α_A and α_P vary in a homologous series, we expect Q to depend on the ratio (α_A/α_P) and we assume

$$Q = Q^*(\alpha_A/\alpha_P) \tag{6}$$

where Q^* is a constant chosen such that $Q<1$ in the entire series. Since α_P increases more rapidly than α_A with the chain length, (α_A/α_P) decreases moderately, and leads to results which can be compared with experimental data.

2.2. *Free energy and order parameters*

The smectic interaction parameter is assumed to be $U_o\alpha$ with $U_o = 4{\cdot}541 \times 500\, k_B$ which corresponds numerically to the Maier–Saupe value used in our earlier paper [22]. The medium is assumed to consist of a mixture of A-type pairs and P-type pairs. Extending the McMillan theory for mixtures, the potential energy of the i^{th} A-type of pair can be written as

$$U_{Ai} = -U_o\alpha_A\tau_A X_A \cos\left(\frac{2\pi Z_i}{d}\right)_A - U_o\alpha_{AP}\tau_p X_p \cos\left(\frac{2\pi Z_i}{d}\right)_A \tag{7}$$

where X_A, X_P, and τ_A, τ_p are the mole fractions, and translational order parameters of the A- and P-type of pairs, respectively, and d the layer spacing given by $X_A d_A + X_P d_P$, with $d_A = r_o + 2c$ and $d_P = r_o + c$. Similarly for a P-type pair, U_{Pj} is obtained by interchanging suffixes A and P in equation (7). Now, the internal energy of one mole of the pairs can be written as

$$2U = \frac{NX_A}{2}\langle U_{Ai}\rangle + \frac{NX_p}{2}\langle U_{Pj}\rangle - NX_P\Delta E \tag{8}$$

where $\langle\rangle$ indicates a statistical average, and the factor 2 on the left-hand side reminds us that we have a mole of pairs. We have also added the concentration dependent part of the configurational energy. N is the Avogadro number.

The molar entropy is given by

$$2S = -Nk\left[X_A\int f_{Ai}\ln f_{Ai}\,dZ_{Ai} + X_P\int f_{Pj}\ln f_{Pj}\,dZ_{Pj}\right] - Nk(X_A\ln X_A + X_P\ln X_P) \tag{9}$$

where the last term is the entropy of mixing, f_A and f_P are the distribution functions of the A- and P-type of pairs respectively. The Helmholtz free energy is given by

$$F = U - TS. \tag{10}$$

The order parameters are given by

$$\tau_A = \int_o^1 \cos(\pi Z')\, f_A\, dZ' \tag{11}$$

where the reduced co-ordinate $Z' = (2Z_i/d)_A$ is used. τ_P is obtained by interchanging suffixes A and P in equation (11). The distribution functions f_A and f_P are found by minimizing F. The normalized distribution function f_A is

$$f_A = \frac{\exp\left[\frac{U}{kT}(\alpha_A X_A\tau_A + \alpha_E X_P\tau_p)\cos(\pi Z')\right]}{\int_o^1 \exp\left[\frac{U}{kT}(\alpha_A X_A\tau_A + \alpha_E X_P\tau_p)\cos(\pi Z')\right]dZ'}. \tag{12}$$

As usual, f_P is obtained by interchanging suffixes A and P in equation (12). Finally, the internal energy per pair can be written as

$$\frac{2U}{N} = -\frac{U_o}{2}[X_A^2\alpha_A\tau_A^2 + X_P^2\alpha_P\tau_P^2 + 2X_AX_P\alpha_E\tau_A\tau_P] - X_P\Delta E \tag{13}$$

and the Helmholtz free energy per pair,

$$\frac{2F}{N} = \frac{U_o}{2}[X_A^2\alpha_A\tau_A^2 + X_P^2\alpha_P\tau_P^2 + 2X_AX_P\alpha_E\tau_A\tau_p] - X_P\Delta E - kTX_A\ln\left(\frac{Z_{\tau A}}{X_A}\right) - kTX_P\ln\left(\frac{Z_{\tau P}}{X_P}\right) \tag{14}$$

where $Z_{\tau A}$ is the partition function given by the denominator of equation (12). $Z_{\tau P}$ is a similar partition function for the P-type of pairs.

The equilibrium value of mole fraction X_A of the A-type of pairs is found by minimizing F with respect to X_A, to get

$$X_A = \frac{1}{1+RX} \tag{15}$$

where

$$RX = \frac{X_P}{X_A} = \frac{Z_{\tau P}}{Z_{\tau A}}\exp\left(\frac{\Delta E}{kT}\right). \tag{16}$$

2.3. *Specific heat at constant volume*

The molar specific heat at constant volume is given by $C_v = [\partial U/\partial T]_v$. Hence the specific heat per pair at constant volume can be written as

$$\frac{2C_v}{N} = -U_o\left\{\frac{\partial X_A}{\partial T}[X_A\alpha_A\tau_A^2 - X_P\alpha_P\tau_P^2 + \alpha_E\tau_A\tau_P(X_P - X_A)]\right.$$

$$+\frac{\partial\tau_A}{\partial T}[X_A^2\alpha_A\tau_A+\alpha_E X_A X_P\tau_p]$$

$$+\frac{\partial\tau_P}{\partial T}[X_P^2\alpha_P\tau_P+\alpha_E X_A X_P\tau_A]\Bigg\}+\frac{\partial X_A}{\partial T}\Delta E. \quad (17)$$

As discussed earlier, ΔE is written as a function of temperature for the sake of convenience in calculation. But, as described in the introduction, ΔE is truly a function of intermolecular separation or equivalently, the volume of the system. Hence, in calculating C_v, where the volume is held fixed, ΔE is not differentiated with respect to temperature.

Expressions for $\partial X_A/\partial T$, $\partial\tau_A/\partial T$ and $\partial\tau_P/\partial T$, are obtained by differentiating with respect to T the equation (15) defining X_A, and equation (11) defining the order parameter. The three derivatives are obtained by solving the three simultaneous equations. It is necessary to calculate the statistical averages $\langle\cos^2(2\pi Z/d)_A\rangle$ and $\langle\cos^2(2\pi Z/d)_P\rangle$ for this purpose.

3. Calculations

We use $Q<1$ i.e. $\alpha_E<\alpha_A\alpha_P$, as explained earlier. At any reduced temperature T_R, consistent values of τ_A and τ_P are found as X_A is varied from 0 to 1 for the assumed set of the four parameters of the problem, namely R_1^*, R_2, α_A and Q^*. Calculations have been made for $R_1^*=8$ and R_2 around 0·7 which are very reasonable values [20]. We evaluate all the necessary integrals numerically by using a 32 point Gaussian quadrature method in double precision. Cramer's rule is used to solve the simultaneous equations involved in the calculation of derivatives required for finding C_v.

We look for the following types of solutions: (1) $\tau_A=\tau_P=0$ corresponding to the nematic phase, and (2) τ_A, $\tau_P\neq 0$ corresponding to smectic phase which is SmA_1 if X_A is small and SmA_d if X_A is large.

4. Results and discussions

4.1. SmA_1–SmA_d transition and critical point C_1

Choosing $Q^*=0{\cdot}22$ and $R_2=0{\cdot}7$, a phase diagram is obtained in which a first order SmA_1–SmA_d boundary ends at a critical point C_1 as α_A is decreased (figure 2). For higher values of α_A, the structural dissimilarity between A-type of pairs and P-type of pairs is large, leading to a large negative deviation from the GM rule, i.e. the mutual interaction between A-type of pairs and P-type of pairs is relatively weak. Hence the 'middle' concentrations of X_A become less stable and this causes a hump in the variation of the free energy with respect to X_A resulting in two minima. This is shown in figure 3 for $\alpha_A=1{\cdot}1$. At $T_R\approx 0{\cdot}6383$, the two minima in free energy become equal resulting in a first order SmA_1–SmA_d transition with a jump in X_A. The latter along with the jumps in the order parameters are shown in figure 4. In the narrow range of temperatures around $T_{A1\text{–}Ad}$ shown in the figure 4 the order parameter τ_p does not have an appreciable dependence on temperature. Over a wider range, τ_p generally decreases with increase of temperature.

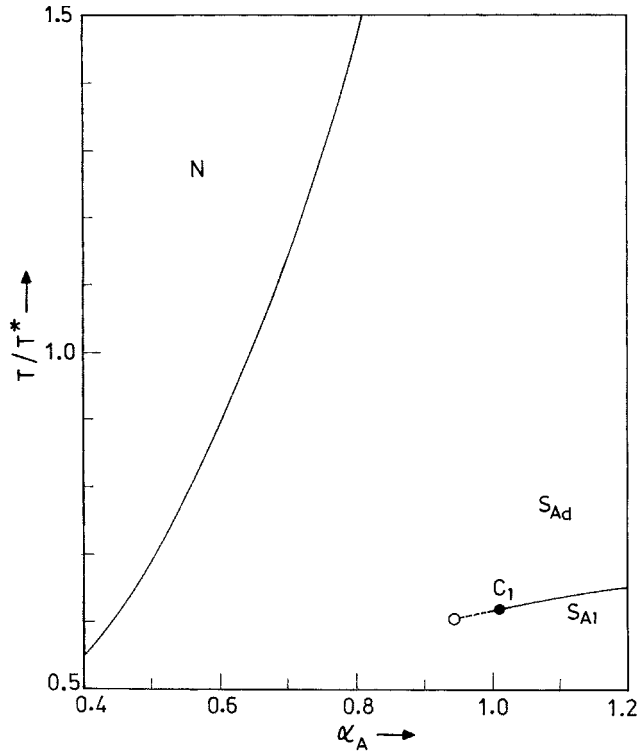

Figure 2. Calculated phase diagram showing the SmA_1–SmA_d critical point C_1 for $R_1^*=8$, $R_2=0{\cdot}7$ and $Q^*=0{\cdot}22$. The open circle shows the critical point which is shifted to a lower value of α_A when $Q^*=0{\cdot}2$.

As α_A is decreased, the dissimilarity between A and P-types of pairs is reduced. Hence the SmA_1–SmA_d transition becomes weaker and at a specific value of α_A ($\approx 1{\cdot}01$) the first order SmA_1–SmA_d line ends in a critical point C_1 for $T_R=0{\cdot}62238$. As the critical point is reached, as expected, the jumps in X_A, τ_A, τ_P and the internal energy approach zero. Correspondingly the specific heat (C_v) becomes stronger and finally diverges at the critical point (see figures 5 to 9). If a lower value of Q is used keeping R_1^* and R_2 fixed, the critical point C_1 of the SmA_1 to SmA_d transition is shifted to lower values of α_A. This is shown by a dashed line in figure 2 for $Q^*=0{\cdot}2$ for which C_1 is at $\alpha_A=0{\cdot}945$ and $T_R=0{\cdot}60867$.

4.2. SmA_1–SmA_d transition and critical point C_2

A further lowering of Q results in other interesting results. With $Q^*=0{\cdot}19$, we have extended the calcu-

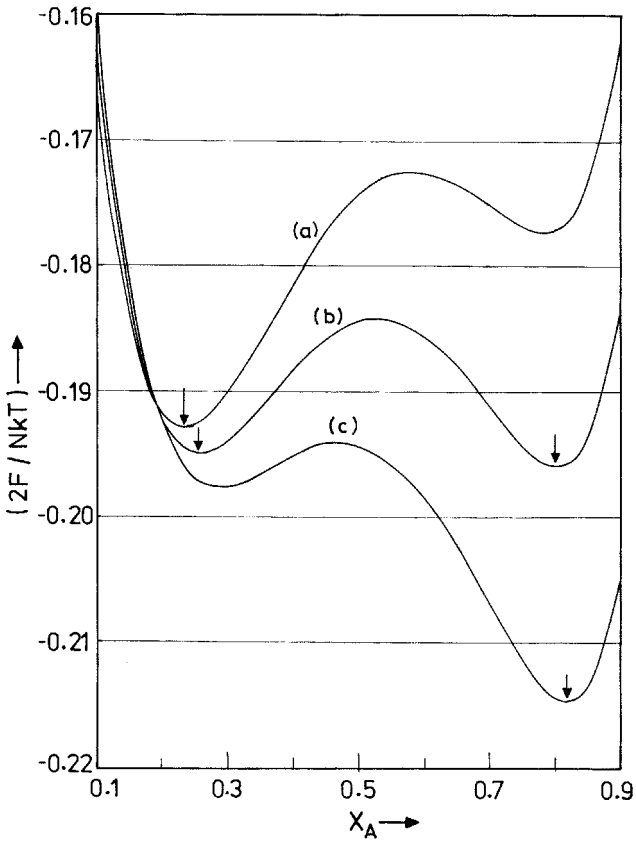

Figure 3. Molar Helmholtz free energy difference ($F_{\text{smectic}}-F_{\text{nematic}}$) as a function of relative concentration of the A-type of pairs (X_A) at three temperatures near T_{A1-Ad} for $R_1^*=8$, $R_2=0{\cdot}7$, $Q^*=0{\cdot}22$ and $\alpha_A=1{\cdot}1$. (*a*) $T/T^*=0{\cdot}6373$, (*b*) $T/T^*=0{\cdot}6383$ and (*c*) $T/T^*=0{\cdot}6393$. The arrows indicate the absolute minima.

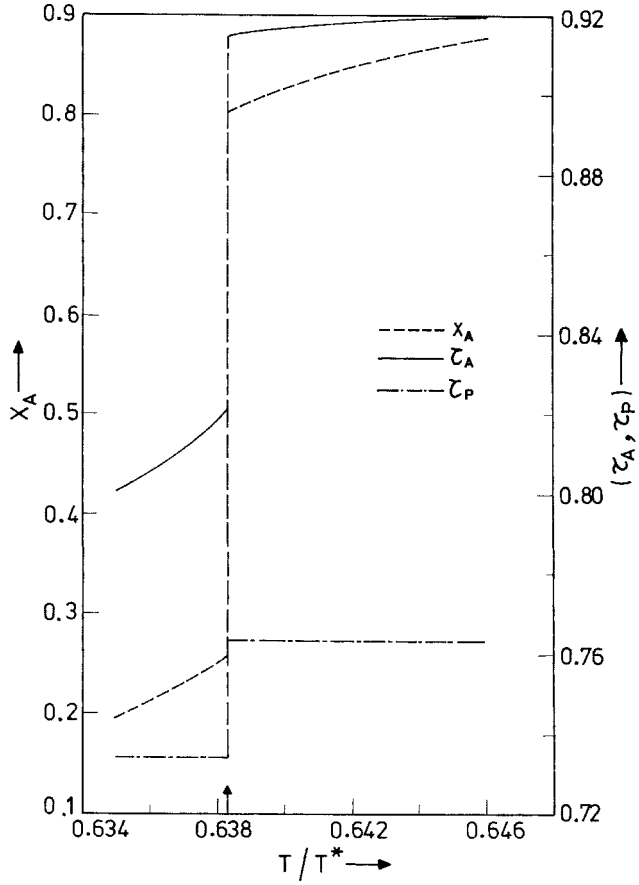

Figure 4. Relative concentration of the A-type of pairs (X_A), smectic order parameter for the A-type of pairs (τ_A) and for P-type of pairs (τ_P) as functions of T/T^* near $T_{A1-Ad}/T^*=0{\cdot}6383$. Other parameters are the same as in figure 3.

lations for α_A values much lower than that corresponding to C_1.

At some low value of α_A, the SmA_1–SmA_d transition *reappears* below another critical point C_2 (see figure 10). This can be understood as follows. At any given value of T_R, ΔE decreases rapidly as α_A is decreased, since the former varies as α_A^4. Also the ratio α_A/α_p which is >1 increases thus stabilizing the A-type configuration. Hence X_A has a relatively large value even at low temperatures with $T_R < R_2$. However as the temperature is further decreased, ΔE becomes sufficiently strong to lower the value of X_A. As seen in figure 11 a sharp variation of X_A with T_R occurs at temperatures T_R considerably lower than R_2 when α_A has a low value, whereas it occurs at $T_R \approx R_2$ for high values of α_A. Since ΔE is small for low values of α_A, the free energy does not vary much over a wide range of X_A. If the GM rule is assumed to be valid (i.e. $Q=1$), the free energy has a shallow minimum with respect to X_A for lower values of α_A while it has a deeper minimum for larger values of α_A. Hence, at low values of α_A, even a small negative deviation from the GM rule is sufficient to cause a 'hump' in the free energy minimum, resulting in two minima with respect to X_A. This leads to a SmA_1–SmA_d transition. Therefore, even though the deviation from the GM rule (i.e. $1-Q$) decreases as α_A is decreased in our calculations, a SmA_1–SmA_d transition appears below some value of α_A, i.e., below another critical point C_2. If the negative deviation from the GM rule is stronger (i.e. Q is lowered), the critical point C_2 is shifted to higher values of α_A. For $Q^*=0{\cdot}19$, C_2 is at $\alpha_A=0{\cdot}385$ and $T_R \approx 0{\cdot}1693$, where as for $Q^*=0{\cdot}18$, C_2 is at $\alpha_A \approx 0{\cdot}43$ and $T_R \approx 0{\cdot}2316$. In general as Q is lowered, both C_1 and C_2 tend to approach each other. For a sufficiently low value of Q we can expect them to merge. But, much before this happens, a nematic lake appears in the middle which is discussed below.

4.3. *Re-entrant nematic lake*

When Q^* is lowered to 0·188, the nematic phase just re-enters over a narrow range of α_A (between 0·585 and

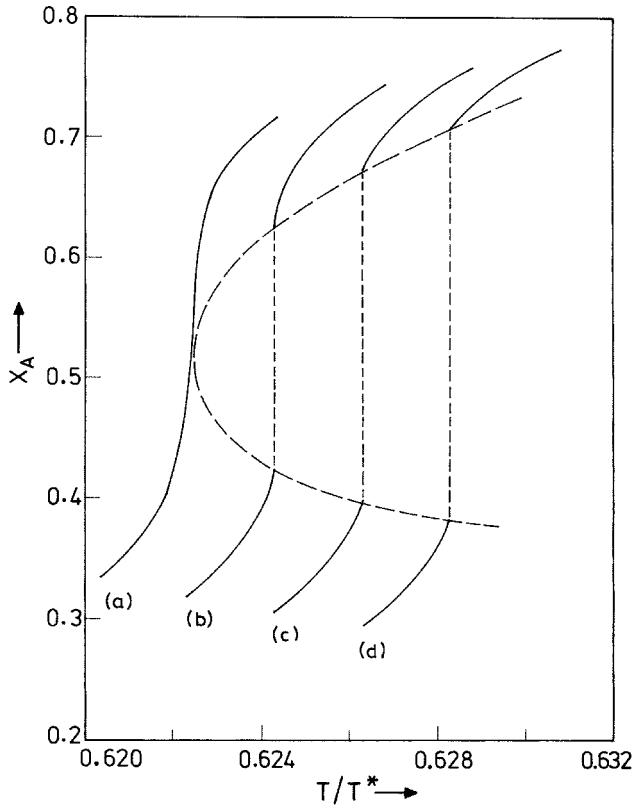

Figure 5. Relative concentration of the A-type of pairs (X_A) as a function of T/T^* near the critical point C_1 of figure 2 for $R_1^* = 8$, $R_2 = 0{\cdot}7$, $Q^* = 0{\cdot}22$ and (*a*) $\alpha_A = 1{\cdot}01$, (*b*) $\alpha_A = 1{\cdot}02$, (*c*) $\alpha_A = 1{\cdot}03$, (*d*) $\alpha_A = 1{\cdot}04$.

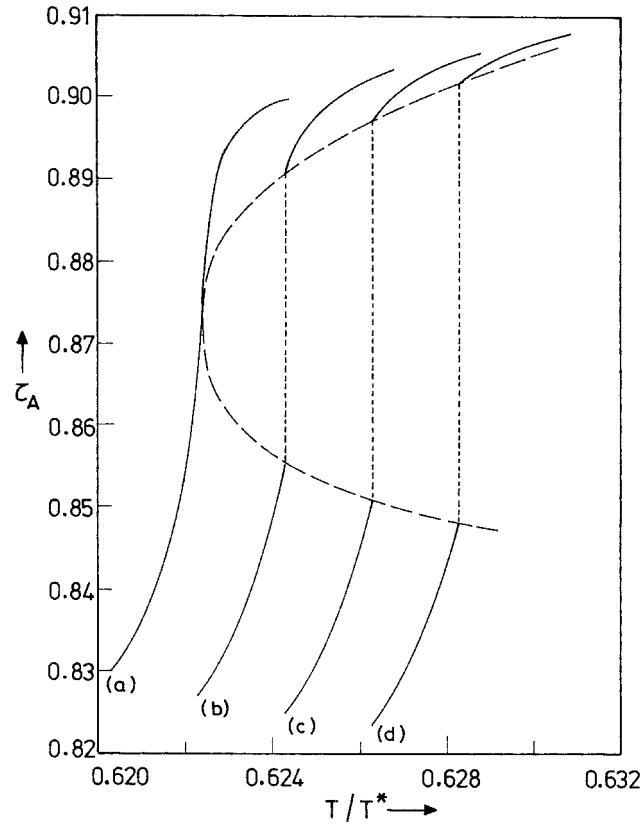

Figure 6. Smectic order parameter of the A-type of pairs (τ_A) as a function of T/T^* near the critical point C_1 of figure 2. The parameters used for calculations of (*a*) to (*d*) are the same as in figure 5.

0·593) and that of temperature (T_R between 0·352 and 0·358). On lowering Q^* to 0·18, the R_N phase widens as a lake occupying larger ranges of α_A and temperature (see figure 12). This can be understood as follows.

In a binary mixture of polar compounds, since the ΔE values of the components are different, the average ΔE per pair can be expected to change with composition. As explained earlier, in our model, α_A is taken to represent a given concentration and ΔE is assumed to vary as α_A^4. Therefore, ΔE is very low at lower values of α_A. But, as explained in the introduction, the re-entrance of the nematic phase on cooling is due to the rapid changeover of A-type of pairs to P-type of pairs at a temperature not low enough to stabilize the SmA_1 phase. However, when ΔE is very low, as discussed above, and shown in figure 11 this changeover occurs at temperatures low enough for the SmA_1 phase to be stable. Therefore, as the temperature is varied at lower values of α_A, the smectic phase is continuous without the intervening R_N region. On the other hand, at intermediate value of α_A, ΔE is strong enough to bring about the 'A' to 'P' changeover on cooling at a *higher temperature*, thus resulting in double re-entrance. Larger values of α_A also lead to larger values of α_P and hence to the stability of the SmA phase leading again to the disappearance of R_N phase. Hence, the R_N region appears as a lake over a range of intermediate α_A values or equivalently, over a range of concentrations in a mixture. In general, we can see that, in the presence of strong negative deviation from GM rule, the smectic phase is destabilized in the 'middle' concentrations, whereas the 'pure' components at both ends have only smectic phases. Indeed, experiments on binary mixtures show that the R_N-lake appears around a concentration of 50 per cent. Further, the R_N-lake appears in association with the SmA_1–SmA_d boundary in the experimental studies (see figure 3 in [5], figure 1 in [2] and figure 1 in [7]).

A further increase of the negative deviation ($Q^* = 0{\cdot}15$) obviously widens the R_N-lake and also as discussed earlier, brings the critical points C_1 and C_2 closer (see figure 13). In this case, near the extreme values of α_A the R_N phase occurs below the SmA_d–SmA_1 transition line. For still lower value of Q ($Q^* = 0{\cdot}12$, see figure 14) or when ΔE is increased using a higher value of $R_2 = 0{\cdot}72$,

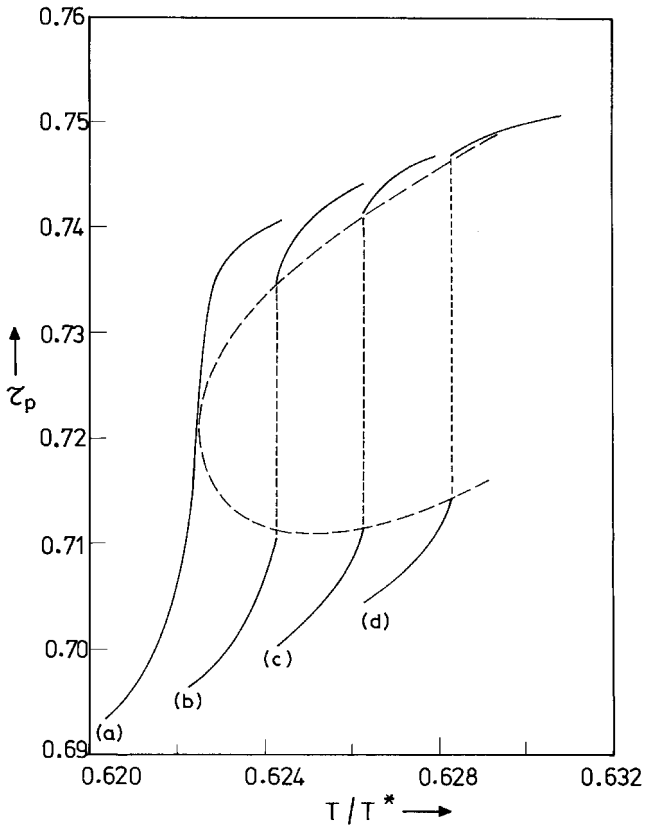

Figure 7. Smectic order parameter of the P-type of pairs (τ_P) as a function of T/T^* near the critical point C_1 of figure 2. The parameters used for calculations of (*a*) to (*d*) are the same as in figure 5.

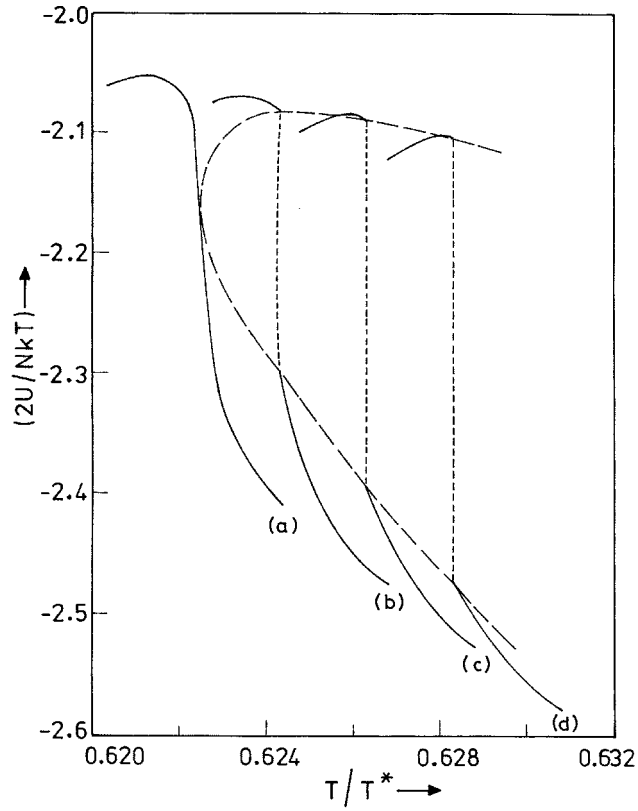

Figure 8. Internal energy per mole of pairs ($2U$) as a function of T/T^* near the critical point C_1 of figure 2. The parameters used for calculations of (*a*) to (*d*) are the same as in figure 5. Note that the temperature variation of ΔE contributes to the positive slope of U in the upper part of the figure.

(see figure 15), the R_N-lake becomes still wider and swallows one or both the SmA_1–SmA_d critical points.

When ΔE is increased further, the nematic lake becomes much wider and eventually merges with the nematic sea creating a 'nematic gap' over a range of α_A between SmA_1 and SmA_d regions (see figure 16). Obviously, the nematic gap widens as Q^* is further decreased or equivalently, the components in a binary mixture become structurally more dissimilar. This agrees with the appearance and widening of the nematic gap in experiments [25] on binary mixtures of compounds exhibiting SmA_1 and SmA_d phases, with the components having various ratios of layer spacing. For a mixture of 7DBT (showing SmA_1) and 8OCB (showing SmA_d), the layer spacing ratio $r = 1{\cdot}46$ and the nematic gap is over a concentration range of $X = 0{\cdot}4$ to $0{\cdot}75$ of 8OCB, whereas for a mixture of 4DBT and 8OCB, $r = 1{\cdot}76$ and nematic gap is between $X = 0{\cdot}3$ to $0{\cdot}9$ (see figure 2 of [25]). Also, we note that the N–SmA_d–R_N boundary is parabolic (see figure 16) which is also seen in the experimental phase diagrams (see figures 2 and 3 of [25]).

Experimentally it is possible to measure the temperature variation of layer spacing. We plot in figure 17 the calculated values of the relative layer spacing $d/d_P = (X_A d_A + X_P d_P)/d_P$ as functions of relative temperature for three values of the McMillan parameter α_A corresponding to the phase diagram shown in figure 13. d shows a maximum value as the temperature is increased in the SmA_d phase. This trend reflects the temperature variation of X_A (see figure 11). The increase in layer spacing from SmA_1 to SmA_d is known [20].

4.4. *Comparison with other theoretical models*

The dislocation loop melting theory developed by Prost and Toner [12] predicts different types of topologies showing a first order SmA_1–SmA_d transition boundary ending at a critical point, the R_N-lake associated with SmA_1–SmA_d transition and the R_N-lake merging with the main nematic sea (see figures 3(*b*), 3(*e*), 5, and 7 of [12]). These topologies are similar to those predicted by our theoretical calculations. Note that, figure 7 of [12] also shows a nematic–nematic transition. But, in the present paper, since the nematic order is assumed to the saturated, such a transition is not possible. However,

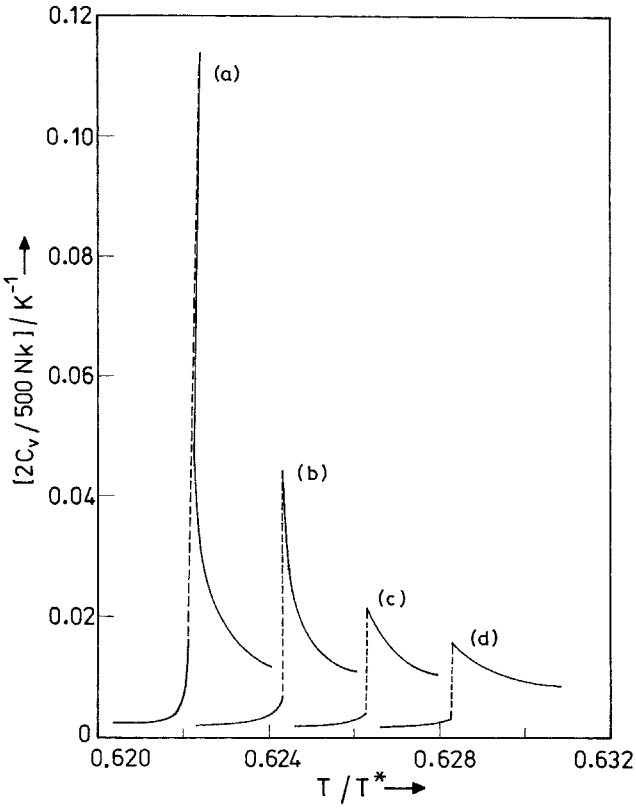

Figure 9. Specific heat at constant volume per mole of pairs ($2C_v$) as a function of T/T^* near the critical point C_1 of figure 2. The parameters used for calculations of (*a*) to (*d*) are the same as in figure 5.

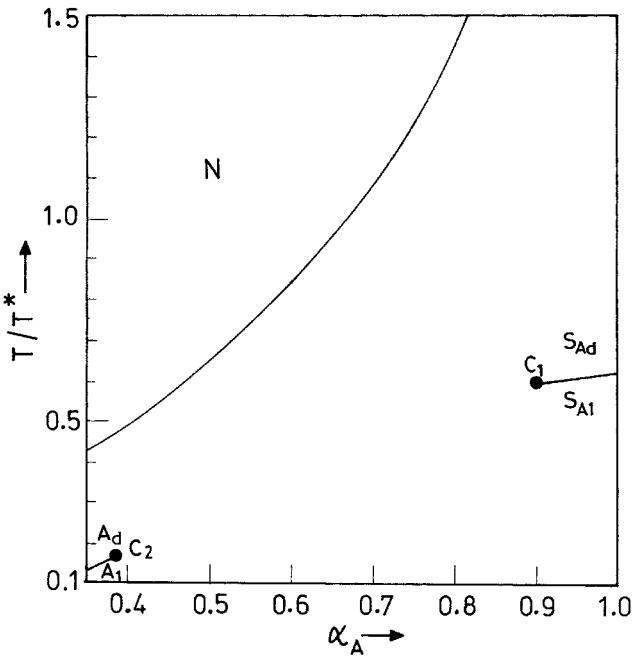

Figure 10. Calculated phase diagram showing two SmA_1–SmA_d critical points C_1 and C_2 for $R_1^* = 8$, $R_2 = 0{\cdot}7$, and $Q^* = 0{\cdot}19$.

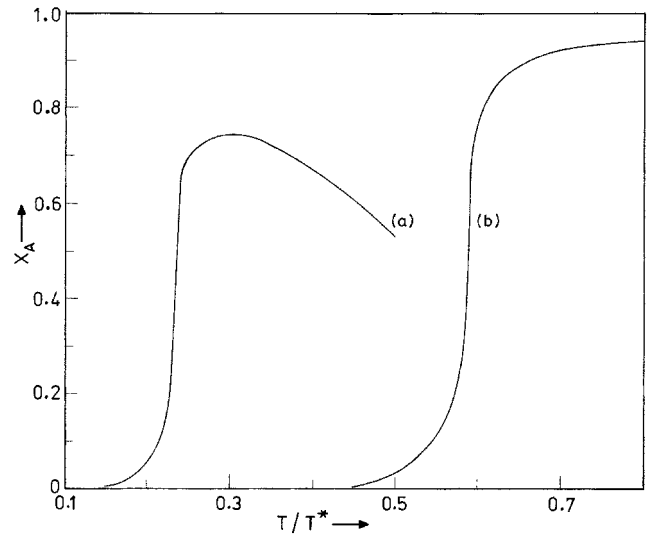

Figure 11. Relative concentration of the A-type of pairs (X_A) plotted as a function of T/T^* for $R_1^* = 8$, $R_2 = 0{\cdot}7$, $Q^* = 0{\cdot}18$ and (*a*) $\alpha_A = 0{\cdot}43$, (*b*) $\alpha_A = 0{\cdot}865$. Note that in (*a*), the rather low value of ΔE leads to a significant *decrease* in X_A as T/T^* is increased beyond 0·3.

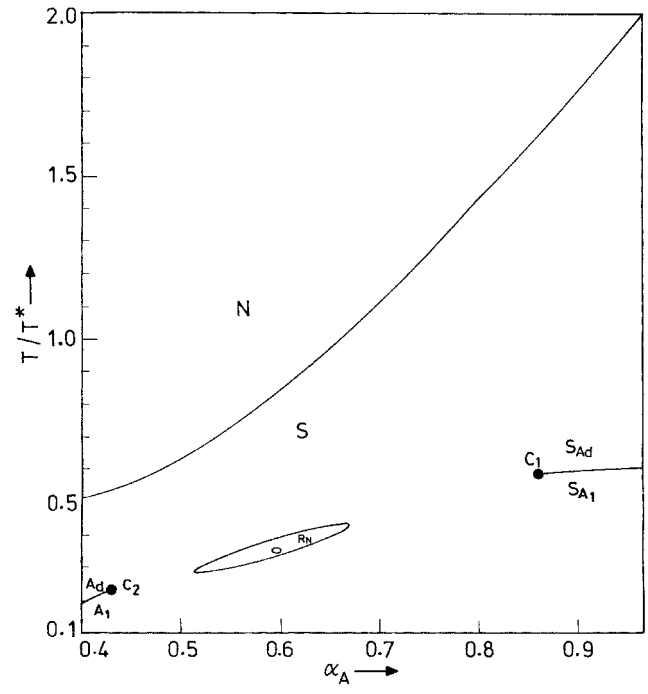

Figure 12. Calculated phase diagram for $R_1^* = 8$, $R_2 = 0{\cdot}7$ showing the re-entrant nematic (R_N) lake for $Q^* = 0{\cdot}18$. The small loop within the R_N lake is for $Q^* = 0{\cdot}188$, for which the R_N lake just begins to appear. C_1 and C_2 are the SmA_1–SmA_d critical points.

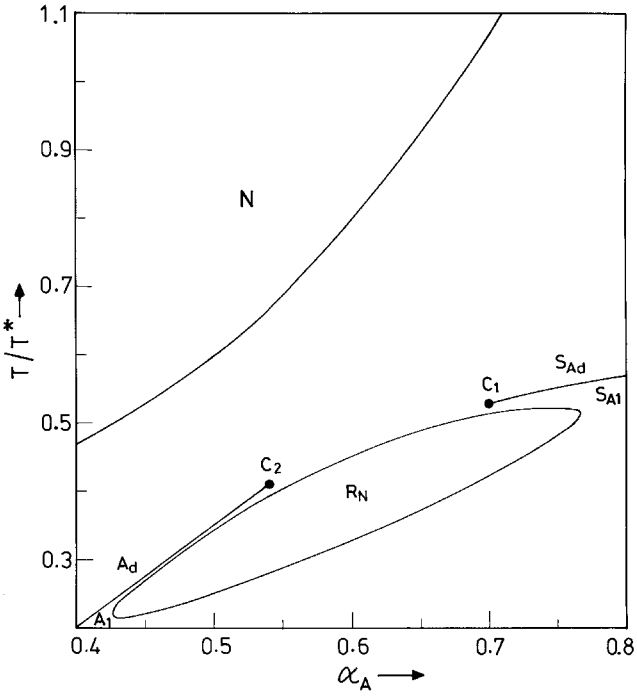

Figure 13. Calculated phase diagram showing a wide re-entrant nematic (R_N) lake for $R_1^* = 8$, $R_2 = 0{\cdot}7$ and $Q^* = 0{\cdot}15$. C_1 and C_2 are the SmA_1–SmA_d critical points.

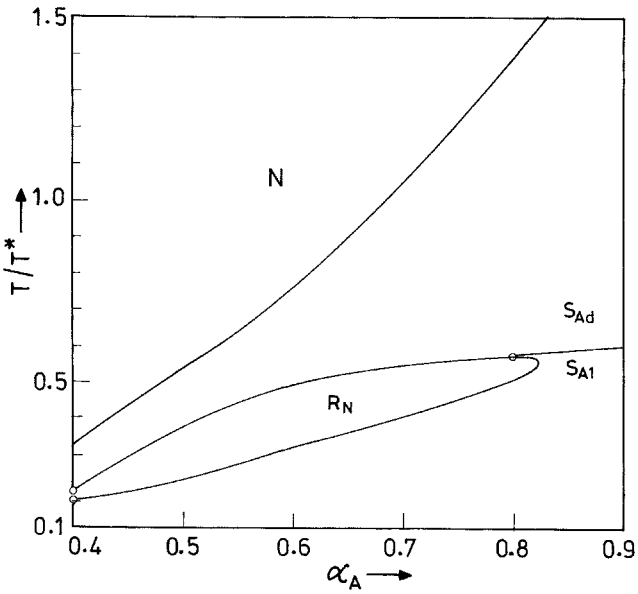

Figure 14. Calculated phase diagram showing a wide re-entrant nematic (R_N) lake for $R_1^* = 8$, $R_2 = 0{\cdot}7$ and $Q^* = 0{\cdot}12$. The point where first order SmA_1–SmA_d transition line meets the boundary of the R_N-lake is shown by the open circle.

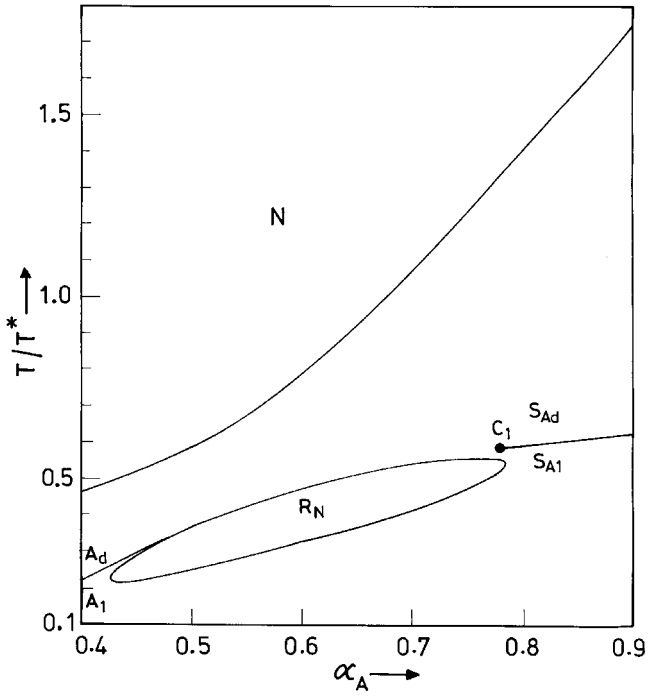

Figure 15. Calculated phase diagram showing a wide re-entrant nematic (R_N) lake for $R_1^* = 8$, $R_2 = 0{\cdot}72$ and $Q^* = 0{\cdot}15$. In this case, the first order SmA_1–SmA_d line merges with the boundary of the lake in the lower range of α_A.

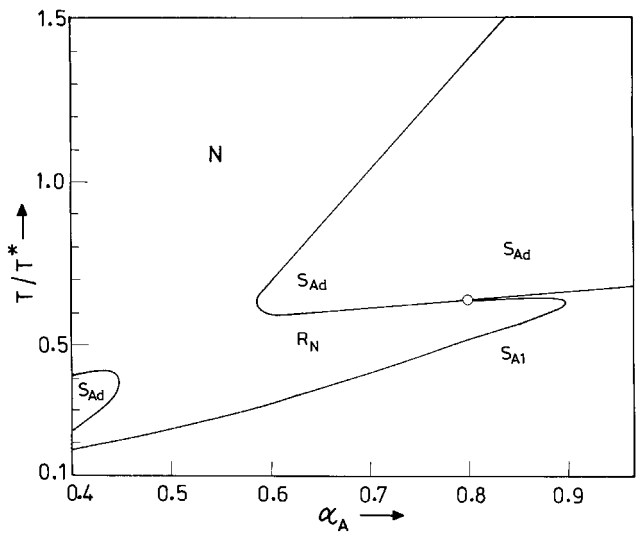

Figure 16. Calculated phase diagram showing the re-entrant nematic (R_N) lake merging with the nematic sea creating a nematic gap, for $R_1^* = 8$, $R_2 = 0{\cdot}75$, $Q^* = 0{\cdot}12$. The open circle indicates the point where the SmA_1–SmA_d transition line meets the R_N boundary.

in our earlier paper [22], in which only nematic interactions were assumed, the possibility of a nematic–nematic transition was predicted. We are extending the theory to include an unsaturated nematic order and the results will be discussed elsewhere.

The microscopic theory using the frustrated spin-gas model developed by Berker *et al.* [26], predicts the possibility of double re-entrance, quadruple re-entrance, SmA_1–SmA_d transition, R_N-lake surrounded by the SmA_d region etc. However, as noted by Garland *et al.*

[8], the R_N-lake predicted by the frustrated spin-gas model does not occur in association with the SmA_1–SmA_d transition where as the experiments [5, 6, 8] and also the Landau theory by Prost and Toner [12] indicate that the R_N-lake occurs in association with the SmA_1–SmA_d transition line and eventually replaces the critical point. This feature is brought out in our molecular model.

The R_N-lake predicted in our model is nearly 'elliptical' with its major axis approximately parallel to the SmA_d–N transition boundary, as seen in the experimental phase diagram [7, 8]. However, the predicted temperature range of the R_N-lake is much larger than the experimental one. It is to be noted that experiments are done on a mixture of two components belonging to different chemical species. Hence, a more detailed theory of mixtures of polar compounds might give results which are in closer quantitative agreement with experimental data.

5. Conclusions

In conclusion, we have used a simple molecular mean field theory of smectics with saturated nematic order and calculated various phase diagrams as functions of model parameters. Our theory explains the phenomenon of double re-entrance, first order smectic A_1 to smectic A_d transition ending at a critical point and the possibility of the appearance of a re-entrant nematic lake associated with the SmA_1–SmA_d transition. The theoretical phase diagrams agree qualitatively with the experimental ones, as well as with the predictions of the dislocation loop model of Prost and Toner. However, the predicted temperature range of the R_N-lake is considerably larger than the experimental one.

We are extending the above theory to include the nematic interactions and to a more general theory of mixtures of polar compounds.

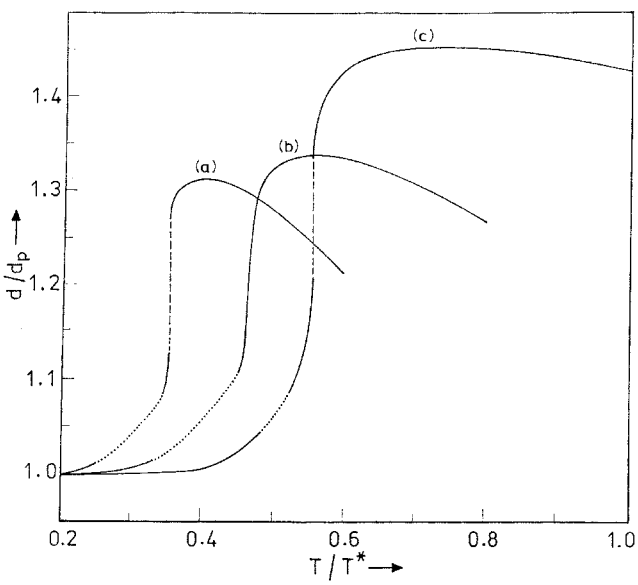

Figure 17. The ratio of average layer spacing d to the molecular length d_P as a function of T/T^* for (*a*) $\alpha_A = 0{\cdot}5$, (*b*) $\alpha_A = 0{\cdot}6$ and (*c*) $\alpha_A = 0{\cdot}75$ corresponding to the phase diagram of figure 13. The dotted lines in the R_N phase represent d values of smectic like short range order. The dashed lines indicate jumps in d at the first order SmA_1–SmA_d transitions.

References

[1] Hardouin, F., Sigaud, G., Achard, M. F., and Gasparoux, H., 1979, *Sol. St. Commun.*, **30,** 265.
[2] Hardouin, F., Levelut, A. M., Achard, M. F., and Sigaud, G., 1983, *J. chim. Phys.*, **80,** 53.
[3] Shashidhar, R., Ratna, B. R., Surendranath, V., Raja, V. J., Krishnaprasad, S., and Nagabhushan, C., 1985, *J. Phys.*, **46,** 4445.
[4] Cladis, P. E., and Brand, H. R., 1984, *Phys. Rev. Lett.*, **52,** 2261.
[5] Hardouin, F., Achard, M. F., Tinh, N. H., and Sigaud, G., 1986, *Mol. Cryst. liq. Cryst. Lett.*, **3,** 7.
[6] Shashidhar, R., and Ratna, B. R., 1989, *Liq. Cryst.*, **5,** 421.
[7] Pfeiffer, S., Heppke, G., Shankar Rao, D. S., and Shashidhar, R., 1992, *Phys. Rev. A*, **46,** R6166.
[8] Wu Lei, Garland, C. W., and Pfeiffer, S., 1992, *Phys. Rev. A*, **46,** 973.
[9] Brodzik, M., and Dabrowski, R., 1995, *Liq. Cryst.*, **18,** 61.
[10] Prost, J., 1980, *Liquid Crystals of One and Two-Dimensional Solids*, edited by W. Helfrich and G. Heppke (Springer, Berlin), p. 125.
[11] Barois, P., Prost, J., and Lubensky, T. C., 1985, *J. Phys.*, **46,** 391.
[12] Prost, J., and Toner, J., 1987, *Phys. Rev. A*, **36,** 5008.
[13] Longa, L., and De Jeu, W. H., 1981, *Phys. Rev. A*, **26,** 1632.
[14] Indekeu, J. O., and Berker, A. N., 1988, *J. Phys.*, **49,** 353.
[15] Dowell, F., 1987, *Phys. Rev. A*, **36,** 5046.
[16] Mirantsev, L. V., 1986, *Mol. Cryst. liq. Cryst.*, **133,** 151.
[17] Katriel, J., and Kventsel, G. F., 1985, *Mol. Cryst. liq. Cryst.*, **124,** 179.
[18] Bose, T. R., Mukherjee, C. D., Roy, M. K., and Saha, M., 1985, *Mol. Cryst. liq. Cryst.*, **126,** 197.
[19] Hida, K., 1981, *J. Phys. Soc. Jap.*, **50,** 3869.
[20] Madhusudana, N. V., and Jyotsna Rajan, 1990, *Liq. Cryst.*, **7,** 31.
[21] Madhusudana, N. V., and Chandrasekhar, S., 1973, *Pramana Suppl.*, **1,** 57.
[22] Govind, A. S., and Madhusudana, N. V., 1993, *Liq. Cryst.*, **14,** 1539.
[23] Humphries, R. L., and Luckhurst, G. R., 1973, *Chem. Phys. Lett.*, **23,** 567.
[24] Demus, D., Fietkau, C. H., Schubert, R., and Kehlen, H., 1974, *Mol. Cryst. liq. Cryst.*, **25,** 215.
[25] Czuprynski, K., Dabrowski, R., Baran, J., Zywocinski, A., Przedmojski, J., 1986, *J. Phys.*, **47,** 1577.
[26] Marko, J. F., Indekeu, J. O., and Nihat Berker, A., 1989, *Phys. Rev. A*, **39,** 4201.